Electric Field Control of Jahn-Teller Distortions in Bulk Perovskites

Julien Varignon,[1,2] Nicholas C. Bristowe,[1,3] and Philippe Ghosez[1]
[1]Physique Théorique des Matériaux, Université de Liège (B5), B-4000 Liège, Belgium
[2]Unité Mixte de Physique, CNRS, Thales, Université Paris Sud, Université Paris-Saclay, 91767, Palaiseau, France
[3]Department of Materials, Imperial College London, London SW7 2AZ, United Kingdom
(Received 23 May 2015; published 1 February 2016)

The Jahn-Teller distortion, by its very nature, is often at the heart of the various electronic properties displayed by perovskites and related materials. Despite the Jahn-Teller mode being nonpolar, we devise and demonstrate, in the present Letter, an electric field control of Jahn-Teller distortions in bulk perovskites. The electric field control is enabled through an anharmonic lattice mode coupling between the Jahn-Teller distortion and a polar mode. We confirm this coupling and quantify it through first-principles calculations. The coupling will always exist within the $Pb2_1m$ space group, which is found to be the favored ground state for various perovskites under sufficient tensile epitaxial strain. Intriguingly, the calculations reveal that this mechanism is not only restricted to Jahn-Teller active systems, promising a general route to tune or induce novel electronic functionality in perovskites as a whole.

DOI: 10.1103/PhysRevLett.116.057602

Perovskite ABO_3 compounds, and related materials, are fascinating systems exhibiting a diverse collection of properties, including ferroelectricity, magnetism, orbital-ordering, metal-insulator phase transitions, superconductivity, and thermoelectricity [1]. Despite the wide range of physical behavior, a common point at the origin of many of them can be identified as being the Jahn-Teller (JT) distortion [2,3]. The Jahn-Teller distortion is, itself, intimately linked to electronic degrees of freedom, since, traditionally, it manifests to remove an electronic degeneracy, opening a band gap and favoring a particular orbital ordering which, in turn, can affect magnetic ordering. Furthermore, it plays an important role, for example, in colossal magnetoresistance phenomena in doped manganites [4], superconductivity [5,6], or the strong electronic correlation observed in the thermoelectric $NaCoO_2$ family [7].

It would be highly desirable, for device functionality, for example, to be able to tune the Jahn-Teller distortion and, hence, its corresponding electronic properties, with the application of an external electric field. However, Jahn-Teller distortions are nonpolar and, hence, not directly tunable with an electric field.

Recently, the concept of "hybrid improper ferroelectricity" has emerged within the community of oxide perovskites [8–11]. This concept is related to an unusual coupling of lattice modes, giving rise in the free energy expansion to a trilinear term $-\lambda PR_1R_2$ linking the polar motion P to two independent nonpolar distortions R_1 and R_2. Such a coupling was identified in various layered perovskites [8,9,12–15], metal-organic framework [16,17], and can even appear in bulk ABO_3 perovskites [18,19]. Interestingly, in Ruddlesden-Popper compounds [9,20] and $ABO_3/A'BO_3$ superlattices [21], this trilinear coupling appeared as a practical way to achieve electric control of nonpolar antiferrodistortive (AFD) motions associated with the rotation of the oxygen octahedra (i.e., monitoring P with an electric field will directly and sizeably tune the nonpolar modes R_1 and/or R_2).

Following this spirit, achieving an electric field control of Jahn-Teller distortions can be realized through the identification of a material exhibiting, by symmetry, a similar "trilinear" term involving both the polarization and the Jahn-Teller distortion which, to the best of our knowledge, has not yet been discovered in bulk ABO_3 perovskites [11]. In the present Letter, we identify such conditions and demonstrate, explicitly, an electric field control in bulk perovskites using a combination of symmetry analysis and first-principles calculations.

The two required lattice distortions are pictured in Figs. 1(a) and 1(b). ABO_3 perovskites often exhibit a nonpolar $Pbnm$ ground state, resulting in a combination of three AFD motions ($a^-a^-c^+$ pattern of rotations of the oxygen octahedra in Glazer's notation [22]). In this symmetry, Howard and Carpenter [23] pointed out that a Jahn-Teller distortion pattern automatically appears, which was later explained in terms of a trilinear coupling with AFD motions [14,24]. As a consequence, a Jahn-Teller distortion is not necessarily electronically driven but can, instead, arise from lattice mode couplings in which case a splitting of the electronic states may develop even in the absence of an electronic instability. The present Jahn-Teller lattice motion corresponds to a Q_2 mode as defined by Goodenough [3], corresponding to two B-O bond length contractions and two B-O elongations. This motion orders at the M point of the Brillouin zone, and hence, consecutive layers along the $\vec{c}$ axis of the $Pbnm$ phase present in-phase distortions. This motion is labelled Q_2^+ throughout the whole Letter.

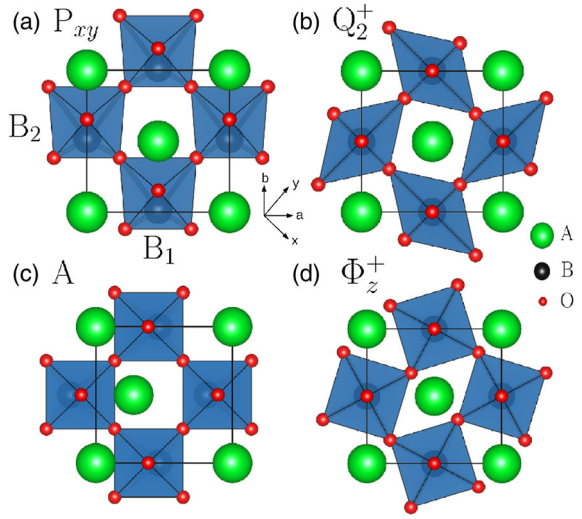

FIG. 1. Schematic view of the main four lattice distortions involved in the $Pb2_1m$ phase of perovskites under tensile epitaxial strain. (a) Polar distortion (irreps Γ_5^-), (b) Q_2^+ Jahn-Teller distortion (irreps M_3^+), (c) antipolar A distortion (irreps M_5^+), (d) $a^0a^0c^+$ ϕ_z^+ antiferrodistortive motion (irreps M_2^+).

Starting from the reference $Pm\bar{3}m$ cubic perovskite phase, the condensation of the polar mode P (irreps Γ_5^-) and the JT mode Q_2^+ (irreps M_3^+) lowers the symmetry to a $Pb2_1m$ phase, a polar subgroup of $Pbnm$. We, then, perform a free energy expansion [25] (around the reference structure) in terms of the lattice distortions allowed by symmetry in this new phase, and we identify, among all the possible terms, some intriguing couplings

$$\mathcal{F} \propto PQ_2^+A + P^2Q_2^+\phi_z^+ + P\phi_z^+A + Q_2^+\phi_z^+A^2. \quad (1)$$

In this phase, the first two terms of Eq. (1) provide a link between the polarization and the Jahn-Teller distortion. These terms also involve two additional distortions: one antipolar A motion pictured in Fig. 1(c) and one $a^0a^0c^+$ AFD motion (labelled ϕ_z^+) pictured in Fig. 1(d). Among all the terms, the lowest order trilinear term of the form PQ_2^+A provides the desired direct coupling between the polarization and the JT distortion. Thus, acting on the polarization with an external electric field may modify the amplitude of the JT motion and, therefore, all related electronic properties.

However, the $Pb2_1m$ symmetry is not the common ground state in bulk perovskites [26]. Strain engineering, through thin film epitaxy, for example, can provide a powerful tool to unlock a polar mode in perovskites [10,27–32]. This is the case for $BiFeO_3$ which was recently proposed to adopt an unusual $Pb2_1m$ symmetry under large epitaxial tensile strain [18,33–35]. This particular phase was shown to develop polar, antipolar, and $a^0a^0c^+$ AFD motions [33], which were later demonstrated to be coupled together through the third term of Eq. (1) [18]. Amazingly, the authors reported the existence of an orbital ordering of the Fe^{3+} $3d$ orbitals, explained from the coexistence of the polar and the antipolar motion yielding a particular lattice distortion pattern [33]. This orbital ordering is unusual since, in this system, no Jahn-Teller effect is required to form a Mott insulating state (Fe^{3+} are in a half filled high spin $t_{2g}^3e_g^2$ configuration). A Jahn-Teller effect or distortion is yet to be reported in the $Pb2_1m$ phase of $BiFeO_3$ to the best of our knowledge. From our symmetry analysis, we clearly demonstrate that, as this $Pb2_1m$ develops the three aforementioned distortions (P, A, and ϕ_z^+), the free energy of Eq. (1) is automatically lowered through the appearance of a fourth lattice distortion: a Jahn-Teller Q_2^+ motion. Therefore, while it may not be unstable itself, the Jahn-Teller motion is forced into the system via this "improper" mechanism arising from the trilinear coupling [8]. This result clarifies the origin of the unusual orbital ordering displayed by $BiFeO_3$; moreover, it provides a pathway to achieve an electric field control of the orbital ordering in bulk perovskites.

The predicted highly strained $Pb2_1m$ phase in bulk perovskites is not restricted to $BiFeO_3$, and it was predicted to occur also in some titanates ($CaTiO_3$ and $EuTiO_3$) [33], in $BaMnO_3$ [33], and even in a Jahn-Teller active compound $TbMnO_3$ [36]. The highly strained bulk perovskites are then an ideal playground to demonstrate our coupling between the polarization and the Jahn-Teller distortion. In order to check the generality of our concept, we propose, in this Letter, to investigate several types of highly strained perovskites on the basis of first principles calculations: (i) nonmagnetic (NM) $SrTiO_3$ ($t_{2g}^0e_g^0$); (ii) magnetic $BaMnO_3$ ($t_{2g}^3e_g^0$) [37], and $BiFeO_3$ ($t_{2g}^3e_g^2$); (iii) Jahn-Teller active $YMnO_3$ ($t_{2g}^3e_g^1$).

First-principles calculations were performed with the VASP package [40,41]. We used the PBEsol [42]+U framework as implemented by Lichtenstein *et al.* [43] (see the Supplemental Material [44] for a discussion on the choice of the U and J parameters). The plane wave cutoff was set to 500 eV, and we used a $6 \times 6 \times 4k$-point mesh for the 20 atom $Pb2_1m$ phase. Projector Augmented Wave pseudopotentials [55] were used in the calculations with the following valence electron configuration: $3s^23p^64s^2$ (Sr), $4s^24p^65s^2$ (Ba), $4s^24p^65s^24d^1$ (Y), $6s^26p^3$ (Bi), $3p^64s^23d^2$ (Ti), $3p^64s^23d^5$ (Mn), $3p^64s^23d^6$ (Fe), and $2s^22p^4$ (O). Spontaneous polarizations were computed using the Berry-phase approach and Phonons, and Born effective charges were computed using the density functional perturbation theory [56]. The electric field effect was modeled using a linear response approach by freezing in some lattice distortion into the system [57,58]. Symmetry mode analyses were performed using the AMPLIMODES software from the Bilbao Crystallographic server [45,46].

We begin by investigating the possibility of a $Pb2_1m$ ground state under large epitaxial tensile strain (the growth

TABLE I. Epitaxial strain (%), magnetic ground state, amplitudes of distortions (Å), and electronic band gap value (eV) for each material. The spontaneous polarization is also reported in $\mu C\,cm^{-2}$. Only the relevant distortions are summarized in the present table [59].

		$SrTiO_3$	$BaMnO_3$	$BiFeO_3$	$YMnO_3$
Strain	(%)	+7.35 [61]	+6.1 [61]	+5.8 [61]	+4.0 [61]
Magnetism		NM	FM	AFMG	AFMG
P (Γ_5^-)	(Å)	0.615	0.421	0.346	0.753
	($\mu C\,cm^{-2}$)	76	45	29	7 [62]
Q_2^+ (M_3^+)	(Å)	0.232	0.190	0.644	0.737
A (M_5^+)	(Å)	0.558	0.217	1.072	0.940
ϕ_z^+ (M_2^+)	(Å)	0.640	0.059	1.668	1.733
Gap	(eV)	3.02	0.28	1.88	1.88

direction is along the [001] axis of the $Pbnm$ structure). Beyond around 5% tensile strain, the four compounds, indeed, develop the desired $Pb2_1m$ ground state. Strained $BaMnO_3$ [ferromagnetic (FM)] and $YMnO_3$ [G-type antiferromagnetic (AFMG)] exhibit a different magnetic ground state compared to the bulk (AFMG and E-type antiferromagnetic, $\uparrow\uparrow\downarrow\downarrow$ zigzag chains coupled antiferromagnetically along the $\vec{c}$ axis, respectively) while $BiFeO_3$ (AFMG) remains in its bulk magnetic ground state. We, then, perform a symmetry mode analysis with respect to a hypothetical $P4/mmm$ phase (corresponding to $Pm\bar{3}m$ for unstrained bulk compounds) in order to extract the amplitude of the relevant lattice distortions [59] (see Table I). As expected, the four materials develop the required distortions, and amazingly, the magnitude of the Q_2^+ Jahn-Teller distortion is relatively large, being, for instance, of the same order of magnitude as the one developed in the prototypical Jahn-Teller system $LaMnO_3$ (around 0.265 Å [60]). Additionally, the values of the spontaneous polarization are rather large, reaching 76 $\mu C\,cm^{-2}$ for $SrTiO_3$, for instance. Despite being highly strained, all materials remain insulating, adopting reasonable electronic band gap values (see Table I).

To shed more light on the origin of this unusual $Pb2_1m$ phase, we compute the energy potentials with respect to the four distortions by individually condensing each mode in a hypothetical $P4/mmm$ phase (see Fig. 2). Surprisingly, the appearance of the $Pb2_1m$ phase is rather different for the four materials. $SrTiO_3$ and $BaMnO_3$ only exhibit a polar instability, producing an $Amm2$ symmetry, consistent with previous reports of a polar phase for these two materials under tensile strain [27,39]. Computing the phonons in this particular $Amm2$ symmetry, only one hybrid unstable phonon mode is identified for these two materials, having a mixed character between the A, ϕ_z^+ and Q_2^+ distortions. For $BiFeO_3$ and $YMnO_3$, the $a^0a^0c^+$ AFD motion is already unstable, which is expected since the $Pb2_1m$ symmetry for these two systems is derived from their bulk $R3c/Pbnm$ phases [59]. Additionally, the JT lattice distortion is also unstable in the $P4/mmm$ phase of $YMnO_3$ and appears as an electronic instability [63], which is expected since $YMnO_3$ is known to be Jahn-Teller active in the bulk. We emphasize, at this stage, that the polar mode in $BiFeO_3$ (and $YMnO_3$) is not unstable, and therefore, highly strained $BiFeO_3$ appears as an improper ferroelectric in contradiction to Ref. [18] (see note [64]). Computing the phonons in the intermediate strained $Pbnm$ phase of both $BiFeO_3$ and $YMnO_3$ compounds reveals only one hybrid unstable mode, having a mixed character between P and A distortions. Despite the apparent universal stability of this highly strained polar phase, the mechanism yielding it is surprisingly different between the compounds and seems linked to the tolerance factor.

Regarding the electronic structure, we checked for the appearance of an orbital ordering as observed in $BiFeO_3$ [33]. For the four compounds, we report the projected density of states on the d levels of two neighboring B sites in the (ab) plane (see Fig. 3). For $SrTiO_3$, a splitting of the t_{2g} states, and especially between the d_{xz} and d_{yz} orbitals,

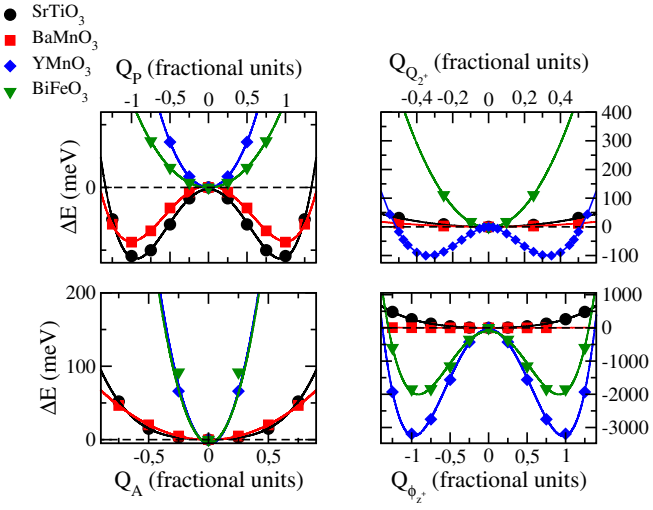

FIG. 2. Potentials with respect to the amplitude of distortions of the four lattice motions producing the required $Pb2_1m$ for $SrTiO_3$ (black filled circles), $BaMnO_3$ (red filled squares), $YMnO_3$ (blue filled diamonds), and $BiFeO_3$ (green filled triangles) starting from the ideal $P4/mmm$ phase.

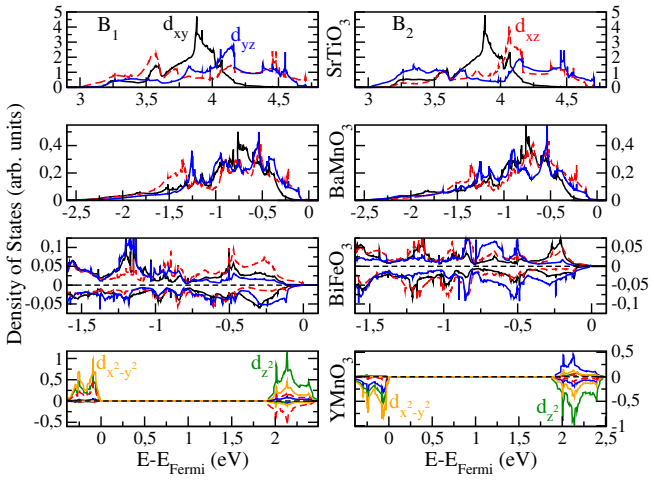

FIG. 3. Projected density of states on the d levels on two neighboring B sites in the (ab) plane of $SrTiO_3$, $BaMnO_3$, $BiFeO_3$, and $YMnO_3$. Local axes of the orbitals are displayed in Fig. 1. The Fermi level is located at 0 eV.

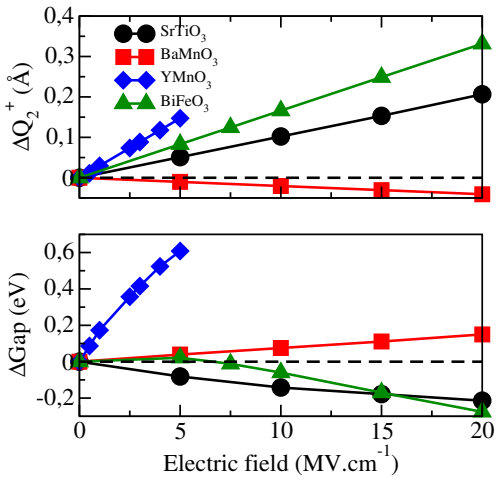

FIG. 4. Electric field effect on the amplitude of the Jahn-Teller distortion (top panel) and the electronic gap value (bottom panel) on the four different compounds.

located at the bottom of the conduction band arises. For $BaMnO_3$ and $BiFeO_3$, a similar splitting between the t_{2g} levels is observed near the Fermi level, even if it is less pronounced for $BaMnO_3$ since it has the smallest Q_2^+ distortion. Finally, $YMnO_3$ displays an orbital ordering of the e_g levels with predominantly $d_{x^2-y^2}$ occupation. This splitting is known to result from the Jahn-Teller distortion in this $A^{3+}Mn^{3+}O_3$ class of material [65]. Additionally, an orbital ordering of the t_{2g} levels is occurring both in the conduction and the valence bands. To prove that the Jahn-Teller distortion, and not another motion, is solely responsible for the orbital ordering, we have condensed all the modes individually and studied the density of states (see Supplemental Material [44], Fig. 1).

Up to this point, we have demonstrated the existence of a JT distortion and a related orbital ordering in the desired $Pb2_1m$ polar phase. Now, we quantify how the trilinear couplings allow us to achieve practical electric field control of the JT distortion. To that end, we compute the magnitude of the JT distortion as a function of the electric field $\vec{E}$, and exemplify its consequences on the electronic band gap. Results are displayed in Fig. 4. The Jahn-Teller distortion is effectively tuned by the application of an electric field along the polar axis through the first and second terms of Eq. (1). As the electric field increases, the amplitude of the JT distortion is either amplified or decreased, being renormalized to around 175% for $SrTiO_3$ for an electric field around 20 MV cm^{-1}. The largest effect is, however, reached for $YMnO_3$ which displays a renormalization of 130% under moderate electric field (around 5 MV cm^{-1}). Therefore, this renormalization of the JT distortion has consequences, for instance, on the electronic band gap value, with an opening or closure around 0.6 eV for $YMnO_3$ or 0.25 eV for $SrTiO_3$. It is then possible, through the coupling between the polarization and the Jahn-Teller distortion, to act on the electronic properties.

Here, we have exemplified a sizeable electric control of the band gap of direct interest for electrochromic and photovoltaic applications. Acting directly on the amplitude of the JT distortion might, alternatively, allow one to control the magnetic state with an electric field, as recently proposed independently in superlattices [14] and metal organic frameworks [16], or to control metal-insulator phase transitions.

In conclusion, we have demonstrated, in the highly strained $Pb2_1m$ phase of bulk ABO_3 perovskites, the existence of a trilinear coupling involving a polar mode and the Jahn-Teller distortion. This improper anharmonic coupling, established on universal symmetry arguments, enables an electric field control of the Jahn-Teller distortion, even in the case of traditionally non Jahn-Teller active systems. The generic mechanism may open novel functionalities in perovskites as it will have consequences on related electronic properties as proposed in the present Letter.

Work supported by the ARC Project TheMoTherm and AIMED and by F. R. S-FNRS PDR Project HiT4FiT. P. G. acknowledges the Francqui Foundation. J. V. aknowledges financial support from the ERC Consolidator Grant No. 615759 MINT. N. C. B. acknowledges support from the Royal Commission of the Exhibition of 1851 and the Junior Research Fellowship scheme at Imperial College London. Calculations have been performed within the PRACE Projects TheoMoMuLaM and TheDeNoMo. They also took advantage of the Céci facilities funded by F. R. S-FNRS (Grant No. 2.5020.1) and Tier-1 supercomputer of the Fédération Wallonie-Bruxelles funded by the Waloon Region (Grant No. 1117545).

J. V. and N. C. B. contributed equally to this work.

[1] P. Zubko, S. Gariglio, M. Gabay, P. Ghosez, and J.-M. Triscone, Annu. Rev. Condens. Matter Phys. **2**, 141 (2011).

[2] H. Köppel, D. R. Yarkony, and H. Barentzen, *The Jahn-Teller Effect* (Springer, New York, 2009).

[3] J. Goodenough, Annu. Rev. Mater. Sci. **28**, 1 (1998).

[4] B. Raveau, M. Hervieu, A. Maignan, and C. Martin, J. Mater. Chem. **11**, 29 (2001).

[5] J. G. Bednorz and K. A. Müller, Rev. Mod. Phys. **60**, 585 (1988).

[6] J. E. Han, O. Gunnarsson, and V. H. Crespi, Phys. Rev. Lett. **90**, 167006 (2003).

[7] R. Berthelot, D. Carlier, and C. Delmas, Nat. Mater. **10**, 74 (2011).

[8] E. Bousquet, M. Dawber, N. Stucki, C. Lechtensteiger, P. Hermet, S. Gariglio, J. M. Gariglio, and P. Ghosez, Nature (London) **452**, 732 (2008).

[9] N. A. Benedek and C. J. Fennie, Phys. Rev. Lett. **106**, 107204 (2011).

[10] J. Varignon, N. C. Bristowe, E. Bousquet, and P. Ghosez, C.R. Phys. **16**, 153 (2015).

[11] N. A. Benedek, J. M. Rondinelli, H. Djani, P. Ghosez, and P. Lightfoot, Dalton Trans. **44**, 10543 (2015).

[12] T. Fukushima, A. Stroppa, S. Picozzi, and J. M. Perez-Mato, Phys. Chem. Chem. Phys. **13**, 12186 (2011).

[13] J. M. Rondinelli and C. J. Fennie, Adv. Mater. **24**, 1961 (2012).

[14] J. Varignon, N. C. Bristowe, E. Bousquet, and P. Ghosez, Sci. Rep. **5**, 15364 (2015).

[15] N. C. Bristowe, J. Varignon, D. Fontaine, E. Bousquet, and P. Ghosez, Nat. Commun. **6**, 6677 (2015).

[16] A. Stroppa, P. Barone, P. Jain, J. M. Perez-Mato, and S. Picozzi, Adv. Mater. **25**, 2284 (2013).

[17] Y. Tian, A. Stroppa, Y.-S. Chai, P. Barone, M. Perez-Mato, S. Picozzi, and Y. Sun, Phys. Status Solidi RRL **9**, 62 (2015).

[18] Y. Yang, J. Íñiguez, A.-J. Mao, and L. Bellaiche, Phys. Rev. Lett. **112**, 057202 (2014).

[19] Q. Zhou and K. M. Rabe, arXiv:1306.1839.

[20] Ph. Ghosez and J.-M. Triscone, Nat. Mater. **10**, 269 (2011).

[21] Z. Zanolli, J. C. Wojdel, J. Iñiguez, and P. Ghosez, Phys. Rev. B **88**, 060102(R) (2013).

[22] A. Glazer, Acta Crystallogr. Sect. B **28**, 3384 (1972).

[23] M. A. Carpenter and C. J. Howard, Acta Crystallogr. Sect. B **65**, 134 (2009).

[24] N. Miao, N. C. Bristowe, B. Xu, M. J. Verstraete, and P. Ghosez, J. Phys. Condens. Matter **26**, 035401 (2014).

[25] D. M. Hatch and H. T. Stokes, J. Appl. Crystallogr. **36**, 951 (2003).

[26] Being in the $Pb2_1m$ phase is *a priori* not mandatory to achieve electric field control of the Jahn-Teller distortions. In a metastable phase, only developing the antipolar A distortion, applying an electric field would activate the polar mode and, through the first term of Eq. (1), the Jahn-Teller distortion may automatically appear. In practice, however, this metastable phase does not seem to be favored, and being in the ground state ferroelectric phase may bring added functionality such as switchable behavior.

[27] J. H. Haeni, P. Irvin, W. Chang, R. Uecker, P. Reiche, Y. L. Li, S. Choudhury, W. Tian, M. E. Hawley, B. Craigo, A. K. Tagantsev, X. Q. Pan, S. K. Streiffer, L. Q. Chen, S. W. Kirchoefer, J. Levy, and D. G. Schlom, Nature (London) **430**, 758 (2004).

[28] J. Junquera and P. Ghosez, J. Comput. Theor. Nanosci. **5**, 2071 (2008).

[29] S. Bhattacharjee, E. Bousquet, and P. Ghosez, Phys. Rev. Lett. **102**, 117602 (2009).

[30] T. Günter, E. Bousquet, A. David, P. Boullay, P. Ghosez, W. Prellier, and M. Fiebig, Phys. Rev. B **85**, 214120 (2012).

[31] C. J. Fennie and K. M. Rabe, Phys. Rev. Lett. **97**, 267602 (2006).

[32] J. H. Lee *et al.*, Nature (London) **466**, 954 (2010).

[33] Y. Yang, W. Ren, M. Stengel, X. H. Yan, and L. Bellaiche, Phys. Rev. Lett. **109**, 057602 (2012).

[34] Z. Fan, J. Wang, M. B. Sullivan, A. Huan, D. J. Singh, and K. P. Ong, Sci. Rep. **4**, 4631 (2014).

[35] In Ref. [33], the space group reported for $BiFeO_3$ under large tensile strain is $Pmc2_1$, which is just an alternative setting of $Pb2_1m$.

[36] Y. S. Hou, J. H. Yang, X. G. Gong, and H. J. Xiang, Phys. Rev. B **88**, 060406 (2013).

[37] While $BaMnO_3$ adopts a hexagonal polar $P63cm$ ground state [38], it can also be stabilized with a perovskite form under tensile strain [39].

[38] J. Varignon and P. Ghosez, Phys. Rev. B **87**, 140403(R) (2013).

[39] J. M. Rondinelli, A. S. Eidelson, and N. A. Spaldin, Phys. Rev. B **79**, 205119 (2009).

[40] G. Kresse and J. Hafner, Phys. Rev. B **47**, 558 (1993).

[41] G. Kresse and J. Furthmüller, Comput. Mater. Sci. **6**, 15 (1996).

[42] J. P. Perdew, A. Ruzsinszky, G. I. Csonka, O. A. Vydrov, G. E. Scuseria, L. A. Constantin, X. Zhou, and K. Burke, Phys. Rev. Lett. **100**, 136406 (2008).

[43] A. I. Liechtenstein, V. I. Anisimov, and J. Zaanen, Phys. Rev. B **52**, R5467 (1995).

[44] See Supplemental Material at http://link.aps.org/supplemental/10.1103/PhysRevLett.116.057602 for details on the computational parameters as well as individual density of states resulting from a mode by mode condensation in $SrTiO_3$, which includes Refs. [36,39,45–54].

[45] D. Orobengoa, C. Capillas, M. I. Aroyo, and J. M. Perez-Mato, J. Appl. Crystallogr. **42**, 820 (2009).

[46] J. Perez-Mato, D. Orobengoa, and M. Aroyo, Acta Crystallogr. Sect. A **66**, 558 (2010).

[47] K. Tsuda and M. Tanaka, Acta Crystallogr. Sect. A **51**, 7 (1995).

[48] F. Kubel and H. Schmid, Acta Crystallogr. Sect. B **46**, 698 (1990).

[49] D. Okuyama, S. Ishiwata, Y. Takahashi, K. Yamauchi, S. Picozzi, K. Sugimoto, H. Sakai, M. Takata, R. Shimano, Y. Taguchi, T. Arima, and Y. Tokura, Phys. Rev. B **84**, 054440 (2011).

[50] D. Lebeugle, D. Colson, A. Forget, and M. Viret, Appl. Phys. Lett. **91**, 022907 (2007).

[51] J. Wang, J. Neaton, H. Zheng, V. Nagarajan, S. Ogale, B. Liu, D. Viehland, V. Vaithyanathan, D. Schlom, U. Waghmare *et al.*, Science **299**, 1719 (2003).

[52] K. Van Benthem, C. Elsässer, and R. H. French, J. Appl. Phys. **90**, 6156 (2001).

[53] R. Sondená, S. Stolen, P. Ravindran, T. Grande, and N. L. Allan, Phys. Rev. B **75**, 184105 (2007).
[54] J. B. Neaton, C. Ederer, U. V. Waghmare, N. A. Spaldin, and K. M. Rabe, Phys. Rev. B **71**, 014113 (2005).
[55] P. E. Blöchl, Phys. Rev. B **50**, 17953 (1994).
[56] S. Baroni, S. de Gironcoli, A. Dal Corso, and P. Giannozzi, Rev. Mod. Phys. **73**, 515 (2001).
[57] J. Íñiguez, Phys. Rev. Lett. **101**, 117201 (2008).
[58] J. Varignon, S. Petit, A. Gellé, and M. B. Lepetit, J. Phys. Condens. Matter **25**, 496004 (2013).
[59] In Table I, we only report the distortions relevant to the proposed mechanism. Notice that, due to a small tolerance factor, $BiFeO_3$ and $YMnO_3$ still develop large $a^-a^-c^0$ rotations in their ground state, in addition to other antipolar modes. Their $Pb2_1m$ phase may appear to be derived from a $R3c$ or $Pbnm$ structure, respectively.
[60] J. H. Lee, K. T. Delaney, E. Bousquet, N. A. Spaldin, and K. M. Rabe, Phys. Rev. B **88**, 174426 (2013).
[61] The strain amplitude is defined with respect to the average in-plane pseudocubic lattice parameters of the fully relaxed ground state structure of each compound as given in the Supplemental Material [44].
[62] Despite a polar mode amplitude in strained $YMnO_3$ larger than in the other compounds, the polarization is much smaller. This is due to the specific atomic pattern of the polar mode in $YMnO_3$: the A and B cations move in opposite directions with similar magnitudes while O motions nearly cancel each other, resulting in a weak polarization. For the three other compounds, both A and B cations move in opposite direction to O anions, maximizing the polarization.
[63] The JT distortion in $YMnO_3$ results from an electronic instability in the high symmetry phase. Indeed, only removing the symmetry on the electronic wave function while keeping the centrosymmetric positions for the cations already produces an energy gain and a lowering of symmetry that is then amplified by the resulting JT lattice distortions.
[64] In Ref. [18], the authors report a weak polar instability in the $P4/mmm$ phase that we do not observe. This may be related to technical details or the magnitude of the strain applied and does not affect the present discussion.
[65] The two average ab plane Mn-O bond lengths are $\langle d_{\mathrm{MnO}}\rangle_{ab,1} = 1.903$ Å and $\langle d_{\mathrm{MnO}}\rangle_{ab,2} = 2.438$ Å while the average Mn-O bond length along the c axis is $\langle d_{\mathrm{MnO}}\rangle_{c} = 1.900$ Å. Consequently, the $d_{x^2y^2}$ orbital should be more stable than the d_{z^2} orbital. Considering the sole Q_2^+ distortion, the two in-plane Mn-O bond lengths are 2.294 Å and 1.772 Å, while the out-of-plane bond length is 1.769 Å.